$e^{\pm}$ pair Background and Masking System for JLC

T. Tauchi
National Laboratory for High Energy Physics, KEK, Oho, Tsukuba-shi, Ibaraki, 305, Japan

Abstract

The major problem occurring in the interaction region of linear colliders has been found to be the background of $e^{\pm}$ pairs created during the collisions of intense beams. The yield of these pairs is estimated by the ABEL simulation for JLC. A masking system against them is proposed together with an optimization of the location of the nearest final quadrupole magnet.

1 INTRODUCTION

A masking system at the interaction region(IR) was proposed at the first JLC workshop. Its purpose is to shield against the large amount of back-scattered photons created in collisions between the $e^{\pm}$ pairs and the final quadrupole magnet. The probability for the O(10^7) photons to escape from the mask η_{mask} should be less than 10^{-3}, which is geometrically determined by the front aperture of the mask. Most of the escaped photons hit the mask surface on the opposite side, then they enter the detector region. In addition the mask must have enough thickness to absorb the photons, that is, its attenuation coefficient should be less than 10^{-5} for 0.5MeV photons which corresponds to 5cm thickness of tungsten. We required that the acceptable number of photons in the detector region is O(10^2) per collision of bunch train.

In the previous ABEL the pairs were created at zero angle along the beam with transverse momenta acquired only from the kick by the electromagnetic field of the oncoming beam. In this paper we modified the ABEL to generate the pairs at finite inherent angles, which may be larger than the kick angle, by using the real photon approximation. The geometric reduction and the effect of the external field are also implemented in the ABEL.

First we derive the analytic expressions for the integrated cross sections as a function of minimal transverse momentum(p_t°) and minimal creation angle($\theta_{\circ}$) which are relevant parameters for the estimation of background in the detector. Secondly, we explain the ABEL and the various effects which are newly implemented in it. We update a masking system at IR to control these backgrounds. Finally we discuss the background in the vertex detector region.

2 THE ANALYTIC FORMULAS

We consider three incoherent pair creation processes, the Breit-Wheeler (BW: $\gamma\gamma \to e^+e^-$) process, Bethe-Heitler (BH: $e^{\pm}\gamma \to e^{\pm}e^+e^-$) process and Landau-Lifshits (LL: $e^+e^- \to e^+e^-e^+e^-$) process. In the calculations of these cross sections the basic kernel is the same using the equivalent photon approximation[1,2]. For the BW process both photons are real beamstrahlung photons; for the BH process one is real and the other one is virtual; for the LL process both photons are virtual. The partial cross sections with transverse momentum (divided by γm) and outcoming angle $\theta_\circ \leq \theta \leq \pi - \theta_\circ$ are calculated by the convolution of two photon energy spectra, $n_a(y_1), n_b(y_2)$, and the differential cross section for $\gamma\gamma \to e^+e^-$, $\sigma_{\gamma\gamma}(y_1, y_2, c)$, as below.

$$\sigma(x_t^\circ, c_\circ) = g \int_{-c_\circ}^{c_\circ} \int_{y_-}^{1} \int_{y_b}^{1} dc dy_2 dy_1 n_a(y_1) n_b(y_2) \sigma_{\gamma\gamma}(y_1, y_2, c), \tag{1}$$

where y_i and c are the fractional photon energy and $c = \cos\theta$, respectively and g=1/4 for the BW process and 1 for both BH and LL processes. The fractional energy x of the outcoming positron(or electron) to its angle θ is expressed by

$$x = \frac{2y_1 y_2}{y_1(1-c) + y_2(1+c)} \tag{2}$$

As denoted in Eq.1, the integration regions of two photon energies are

$$1 \geq y_1 \geq y_b = \frac{y_2 y_+}{y_2 - y_-}, \quad 1 \geq y_2 \geq y_-, \tag{3}$$

$$y_\pm = \frac{x_\circ}{2}(1 \pm c) = \frac{x_t^\circ}{2}\sqrt{\frac{1 \pm c}{1 \mp c}}, \tag{4}$$

where $x_\circ$ and x_t° are the minimum energy and the minimum transverse energy. These lower bounds are very important for the calculations because the dominant contribution comes from them. The virtual and the beamstrahlung photon spectra are given by

$$n_v(y) = \frac{2\alpha}{\pi}\frac{1}{y}\ln(\frac{1}{y}) \qquad \text{and} \tag{5}$$

$$n_b(y) = \frac{1}{\pi}\Gamma(\frac{2}{3})(\frac{\alpha\sigma_z}{\gamma\lambda_e})(3\Upsilon)^{2/3} y^{-2/3} \equiv A y^{-2/3}, \tag{6}$$

respectively, where σ_z, λ_e and γ are the beam bunch length, the electron Compton wavelength and a Lorentz factor for the beam, respectively. Finally $\sigma_{\gamma\gamma}(y_1, y_2, c)$ is calculated by neglecting the obviously small terms $<$O(γ^{-2}).

$$\sigma_{\gamma\gamma}(y_1, y_2, c) = \frac{\pi r_e^2}{\gamma^2 y_1 y_2}\frac{1}{1-c^2}\left\{\frac{y_1^2(1-c)^2 + y_2^2(1+c)^2}{[y_1(1-c) + y_2(1+c)]^2}\right\} \tag{7}$$

$$\simeq \frac{\pi r_e^2}{\gamma^2 y_1 y_2}\frac{1}{1-c^2}, \tag{8}$$

where r_e is the classical electron radius. The last approximation of Eq.8 is only used in analytic calculations since the value in the parenthesis (Eq.7) varies slowly from 1/2 to 1 and it is well factorized outside of the integral (Eq.1) , which is estimated to be 0.7 with an accuracy of a few % by comparing this approximation and the numerical integration with no such approximation. The resultant integrated cross sections are expressed below as a function of x_t° and $\theta_\circ$, which are already multiplied by the factor of 0.7 in order to compensate the last approximation,

$$\sigma_{\mathrm{BW}}(x_t^\circ, \theta_\circ) = 1.69\frac{r_e^2}{\gamma^2}A^2(\frac{2}{x_t^\circ})^{4/3}\ln\frac{1}{\tau_\circ} \tag{9}$$

$$\sigma_{\mathrm{BH}}(x_t^\circ, \theta_\circ) = 3.55\frac{\alpha r_e^2}{\gamma^2}A(\frac{2}{x_t^\circ})^{5/3}(\tau_\circ^{1/3} - \tau_\circ^{-1/3})(\ln\frac{x_t^\circ}{2} + 0.21) \tag{10}$$

$$\sigma_{\mathrm{LL}}(x_t^\circ, \theta_\circ) = 0.83\frac{\alpha^2 r_e^2}{\gamma^2}(\frac{2}{x_t^\circ})^2\ln\frac{1}{\tau_\circ}(\ln\frac{x_t^\circ}{2\tau_\circ}\ln\frac{x_t^\circ\tau_\circ}{2} + 3\ln\frac{x_t^\circ}{2} + 4.44) \tag{11}$$

where $\tau_\circ = \tan(\theta_\circ/2)$. The above expressions account for only one of the two particles(say positron) of the pair. To count the electron as well, we must multiply each expression by 2.

The above formulas are valid for large inherent angle scattering since they have a collinear singularity which is clearly seen in Eq.8. The reason for this singularity is our neglect of the electron mass(m_e) in the derivation of the formulas. Remembering that the typical scattering angle is m_e/E_e, where E_e is the energy of e^- or e^+ of a pair, the valid angular region will be $\theta > m_e/E_e$. More detailed discussion on how to treat this singularity in event generation will be found in the subsequent sections.

3 THE ABEL SIMULATION

3.1 Event Generation

In ABEL,the beam bunches are described by ensembles of macro-particles. The number of macro-particles is typically 10^3 to 10^5. The whole process is divided into time slices. At each time step the bunches are further divided into longitudinal slices. The modification of ABEL is that the pairs are created in the collision between the macro-particles and the beamstrahlung photons in each longitudinal slice. There is no pair creation between the different slices, that is the incoherent pair creation processes are "local" in the longitudinal direction. Then the created particles(e^+ or e^-) are tracked in the Coulomb potential which is produced by the oncoming beam. As the transverse momenta of these particles are affected by the kick in the tracking, the integrated cross sections for the processes in ABEL are given by $(x_\circ, \theta_\circ)$ instead of $(x_t^\circ, \theta_\circ)$, and there are no integrations over the beamstrahlung photon energy spectra for the BW and BH processes.

$$\sigma_{\mathrm{BW}}(y_1, y_2, \theta_\circ) = 6.28\frac{r_e^2}{\gamma^2}\frac{1}{y_1 y_2}\ln\frac{1}{\tau_\circ} \tag{12}$$

$$\sigma_{\mathrm{BH}}(y_1, \theta_\circ) = 8\frac{\alpha r_e^2}{\gamma^2}\frac{\ln\tau_\circ}{y_1}\left(\frac{\ln y_{min} + 1}{y_{min}} - 1\right) \tag{13}$$

$$y_{min} = max\left(\frac{x_\circ}{2}(1 - c_\circ),\ \ \frac{1}{\gamma^2}\right), \quad c_\circ = \cos\theta_\circ \tag{14}$$

$$\sigma_{\rm LL}(x_\circ,\theta_\circ) = 0.64\frac{\alpha^2 r_e^2}{\gamma^2}(\frac{2}{x_\circ})^2\Big\{(\ln\frac{x_\circ}{2}+1)\{(\ln\frac{x_\circ}{2}+\frac{3}{2})(\frac{c_\circ}{1-c_\circ^2}-\ln\tau_\circ) + \frac{c_\circ\{1+\ln(1-c_\circ^2)\}}{1-c_\circ^2}\}\Big\}, \tag{15}$$

where y_1, y_2 are the beamstrahlung photon energies. For the virtual photon energy, we use the distribution of Eq.5. The energy of the outgoing particle is calculated by Eq.2 with y_1, y_2 satisfying the boundary conditions of Eq.3. The transverse momentum is calculated by the energy and the final scattering angle after the kicks.

For the generation of collinear pairs, a minimum cut-off angle θ_{cut} has to be introduced to regulate the singularity which is mentioned in the previous section, *i.e.* $\theta > \theta_{cut}$. The cut-off angle is a function of $m_e/E_e = 1/x\gamma$ and it depends on the processes of BW,BH,LL as follows,

$$\theta^i_{cut}(x) = f_i\frac{1}{x\gamma}, \qquad i = \mathrm{BW, BH \ or \ LL} \tag{16}$$

where, $f_{\rm BW}, f_{\rm BH}$ and $f_{\rm LL}$ are patch factors to be determined by the normalization of their total cross sections. In addition to these cut-off angles, the energies of two photons must fulfill the following threshold condition of an e^+e^- pair creation which is also ignored in the zero electron mass approximation.

$$y_1 y_2 > \frac{1}{\gamma^2} \tag{17}$$

3.2 Justification of Our Method

The total cross sections for the three processes are well known and are expressed below.

$$\sigma_{\rm BW} = \frac{3}{8}(\ln 4 + \frac{3}{2})\pi r_e^2 \gamma^{-2/3}(L - \ln 4)A^2 \tag{18}$$

$$\sigma_{\rm BH} = \frac{28}{3}\alpha r_e^2(L - \frac{235}{42})A \tag{19}$$

$$\sigma_{\rm LL} = \frac{\alpha^2 r_e^2}{\pi}(\frac{28}{27}L^3 - 6.59L^2 - 11.8L + 104) \tag{20}$$

where $L = \ln 4\gamma^2$, and $\sigma_{\rm BH}, \sigma_{\rm BW}$ are already integrated over the beamstrahlung photon energy spectrum of Eq.6. By comparing values calculated by the above equations and those of the numerical integration of Eq.1 over $\gamma^{-1} < x < 1$ with the cut-off angles and the threshold conditions for the two photon energies, the patch factors are determined to be,

$$f_{\rm BW} = 0.5, \quad f_{\rm BH} = 0.92 \quad \text{and} \quad f_{\rm LL} = 0.7. \tag{21}$$

Table 1: Total cross sections for the three incoherent processes at E_{beam}=500GeV in cm^2.

process	calculations by Eqs.18,19,20	our method numerical integration of Eq.1
BW	1.9×10^{-27}	1.9×10^{-27}
BH	2.7×10^{-25}	2.8×10^{-25}
LL	5.6×10^{-26}	5.2×10^{-26}

The total cross sections thus calculated are summarized in Tab.1 for JLC [5] with E_{beam} = 500GeV, for which A(the cross section) is 1.11. In order to verify our method, the energy(x) distributions for BH and LL are also compared with the known formulas[4] and the results are shown in Fig.1 (a),(b). As is clearly seen in these figures, the agreement between the two is good for the energy region of interest($E_e > 5$MeV).

3.3 Geometric Reduction

The finite impact parameter of the interactions in these processes comes from the transverse energy(q_t) of the virtual photon. The distribution of $y_t(\equiv q_t/\gamma m_e)$ is[4]

$$n_v(y_t) = \frac{y_t^2 dy_t^2}{(y_t^2 + y^2/\gamma^2)^2}. \tag{22}$$

The integral of the above equation corresponds to the logarithmic term of Eq.5, and the range of its integration over y_t is from y/γ^2 to $1/\gamma$. For a given equivalent photon energy y, the dominant contribution to the integration comes from the region of small transverse momentum $y_t \sim y/\gamma$. In ABEL every virtual photon has finite transverse energy(y_t) according to Eq.22. To account for this non-local nature of the virtual photon interaction, we first calculate the probability of pair creation which is proportional to the local intensities of the two beams (macro-particles or beamstrahlung photons) at a point. Defining the impact parameter(ρ) as $1/y_t\gamma m_e$, we get the non-local intensities of two beams separated by ρ from each other, where for the LL process ρ is actually a sum of two impact parameters. Then the reduction factor can be obtained by the ratio of "non-local" intensities divided by the "local" ones. If the separation is far beyond the beam (transverse) size, the pair creations will be suppressed strongly[3]. ABEL creates the pairs at the position separated by ρ from the beam position and even outside the beam size. For analytic calculations, this geometric reduction can be taken into account by limiting the integration region of y_t $(1/\sigma_y\gamma m_e < y_t < 1/\gamma)$ in Eq.22, where σ_y is a transverse beam size at a collision point [6].

3.4 Effect of the Strong External Field

Since the $e^{\pm}$ pairs are created in the external field of the oncoming beam, which is a magnetic field of O(10^3) Tesla at a TeV linear collider such as JLC, cross sections involving virtual photons, σ_{LL} and σ_{BH}, are affected and eventually suppressed by the magnetic field[9]. This effect is well explained by a radiation angle of a virtual photon in a magnetic

[3] This *geometric reduction* effect was first observed at Novosibirsk[7], and subsequently developed theoretically by several authors[6,8].

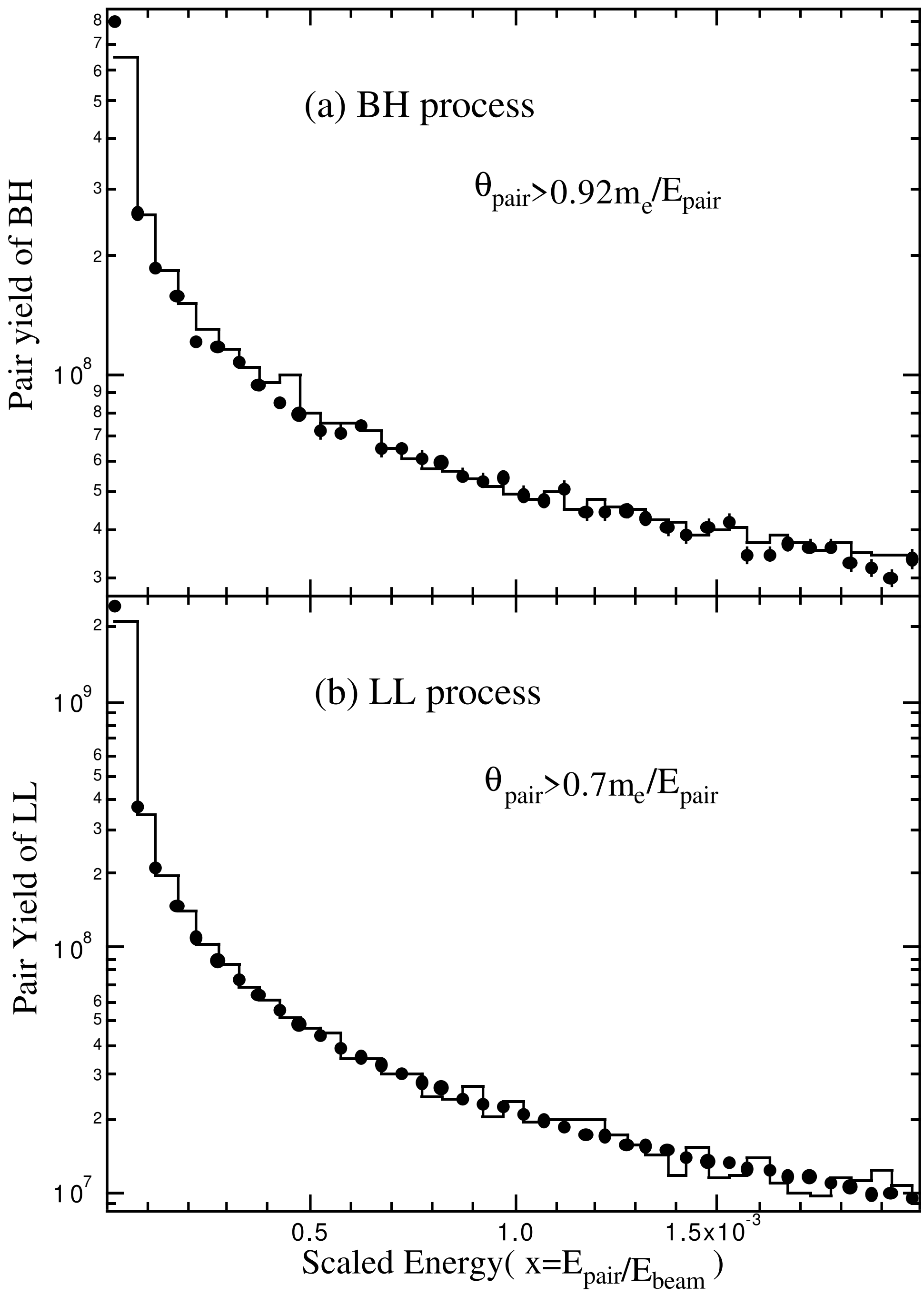

Figure 1: (a)Scaled energy *(x)* distributions of one of pair particles created in the BH process for JLC at $E_{beam} = 500\text{GeV}$. The histogram is given by the known formula and plotted data are given by numerical integration with $f_{\rm BH} = 0.92$. (b) same as (a) for LL process, where $f_{\rm LL} = 0.7$.

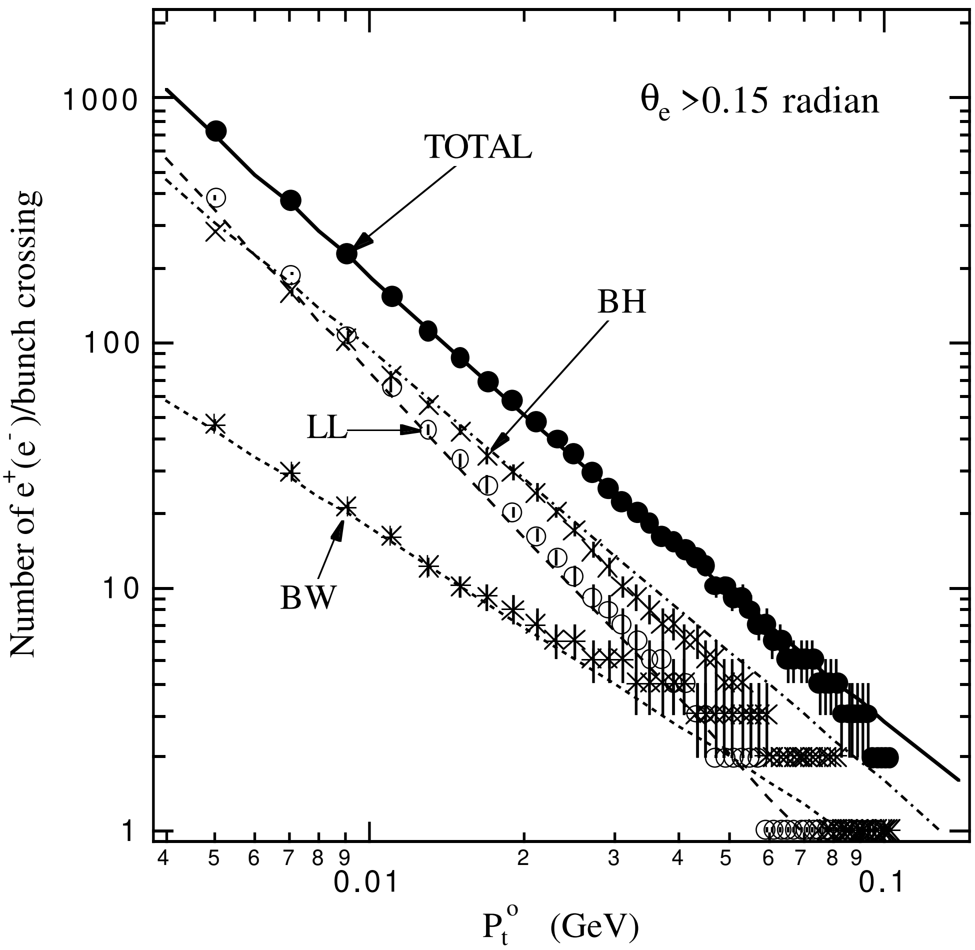

Figure 2: Comparison between the analytic calculation and the ABEL.

field $\theta_H = 1/\gamma(\omega_c/\omega)^{1/3}$, which is compared with the angle in free space $\theta = 1/\gamma$, where ω and ω_c are an energy of the photon and a critical energy of a synchrotron radiation in the magnetic field, respectively. Requiring an inequality of $\theta > \theta_H$, the transverse energy of a virtual photon ω_t has a lower bound given by

$$\omega_t > \omega\theta_H = \frac{\omega}{\gamma}(\frac{\omega_c}{\omega})^{1/3} \quad \text{or} \quad y_t > \frac{y}{\gamma}(\frac{\Upsilon}{y})^{1/3}. \tag{23}$$

Thus the external magnetic field increases the minimal transverse energy transfer. This effect appears as a suppression of the pair creations with large impact parameters similar to geometric reduction. In ABEL the virtual photon participating in pair creation is required to fulfill the above condition(Eq.23) .

3.5 Results

For further study, we list the JLC parameters at beam energies (E_{beam}) of 250, 500 and 750GeV, which are relevant to our calculation, in Tab.2. The total pair yields per bunch crossing are also listed for each process in this table, which are calculated by Eqs.18,19 and 20. In order to see a consistency between the analytic calculations and the ABEL, we plot the yields at E_{beam}=500GeV per bunch crossing, calculated by the cross sections

Table 2: JLC parameters relevant to our calculation and the total pair yields per bunch crossing at E_{beam}=250,500 and 750GeV. The frequency of JLC is 150 Hz(trains/sec) with 20 bunches/train and the bunch separation is 1.4nsec.

E_{beam} (GeV)	250	500	750
L/bunch cm^{-2}	1.1×10^{30}	4.0×10^{30}	5.7×10^{30}
σ_x nm	335.3	372.0	561.3
σ_y nm	4.5	3.1	2.7
σ_z μ m	151.5	112.8	94.6
beam intensity($N_{e^\pm}$/bunch)	1.26×10^{10}	2.02×10^{10}	2.67×10^{10}
$\langle \Upsilon \rangle$	0.085	0.43	0.66
A	1.01	1.11	0.83
total pair yields/bunch			
BW	2.6×10^{3}	7.6×10^{3}	4.7×10^{3}
BH	2.7×10^{5}	1.1×10^{6}	1.2×10^{6}
LL	4.9×10^{4}	2.2×10^{5}	3.3×10^{5}

of Eq.9,10 and 11 and their sum as a function of $p_t^\circ = \gamma m_e x_t^\circ$ at $\theta > 0.15$ together with the results of the ABEL which are plotted with error bars(Fig.2). Major detectors for an experiment are required to be located in this angular region. The yields of the analytic calculations are already multiplied by 2 for e^+ and e^-. In this figure the effects of the kick, the non-local interaction and the external field in ABEL are switched off just for comparison. The agreement for all three processes is very good.

In addition to the large inherent angles of the pair creations, ABEL implements the kick, the geometric reduction and the external field effect as described in the previous section. To see these individual effects in detail, we simulated the pairs under the four kinds of conditions also at E_{beam}=500GeV, that is (a) the only kick is taken into account, (b) the kick and the external field effect are considered, (c) and (d) include all effects, where (a), (b) and (c) have no angular constraints except for Eq.16 and (d) requires the minimal angle $\theta_\circ = 0.1$ of the pair creation in addition. The results are shown in Fig.3, where the total yields summed over the three processes are plotted in the same way as Fig. 2 , together with the total yield calculated by the analytic formulas which is drawn by a solid line. The geometric reduction rate is 70% at $p_t^\circ = 5$MeV and it decreases gradually to 40% at $p_t^\circ > 25$MeV. There is also 40-20% reduction due to the external field effect. However the latter reduction is mostly included in the former one, since these two reductions are due to essentially the same effect on the transverse energy transfer and the geometric one is dominant in the present case of a very small beam spot size. By comparing (c) with (d) in Fig.3, a huge number of pairs for $p_t^\circ < 20$MeV comes from the pairs created at a very forward angle ($\theta << 0.1$), a major part of whose transverse momenta is acquired by the kick. A sharp shoulder seen at about $p_t^\circ = 20$MeV corresponds to the maximum kick angle of these pairs at $\theta > 0.15$. Beyond this shoulder ($p_t^\circ > 20$MeV), the effect of the kick is small and the analytic calculation with the geometric reduction[6] is a good approximation of the ABEL result. Finally figure 4 show the total yields at the three beam energies of 250,500 and 750GeV. The shoulder positions in p_t° are roughly proportional to the beam energy, which will determine the aperture of a mask.

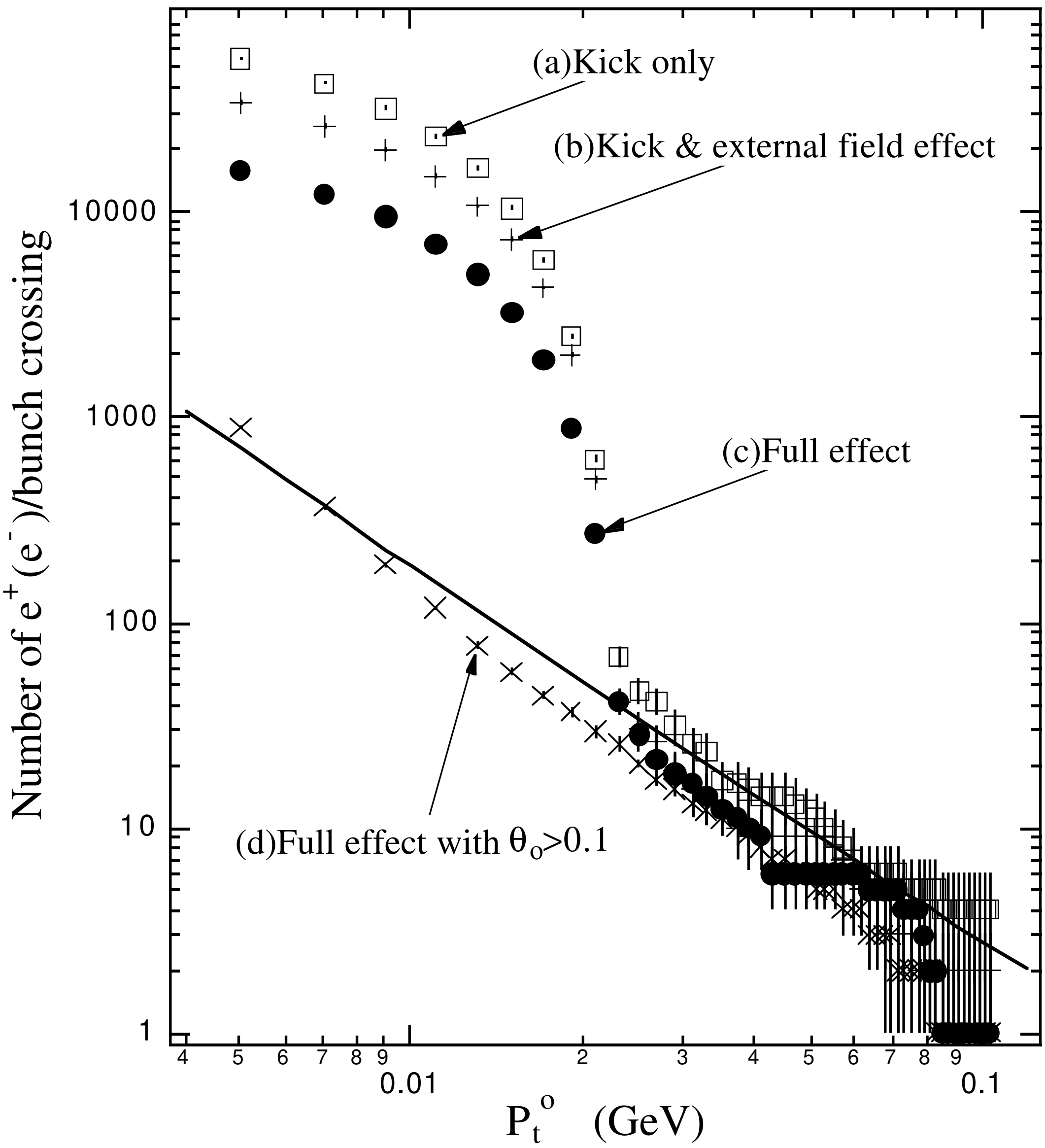

Figure 3: The ABEL simulation results with the various effects of (a)-(d) which are explained in the text. The vertical axis is the number of pair particles(e^+ and e^-) integrated for $p_t > p_t^\circ$ in the angular region of $\theta_e > 0.15$. The solid line expresses the total number calculated by the analytic equation, which is as same as the TOTAL in Fig.2.

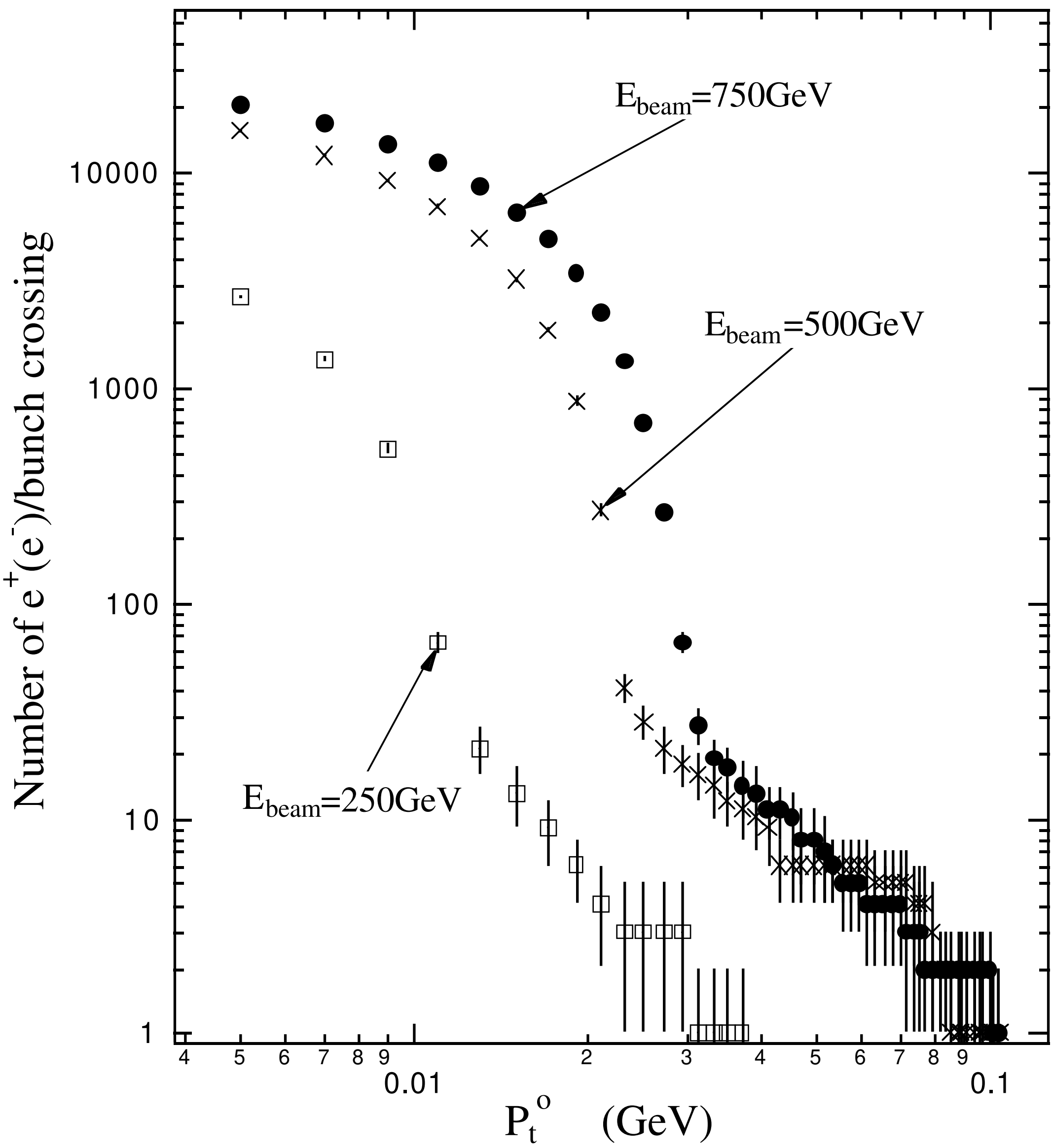

Figure 4: The number of pairs for $p_t > p_t^{\circ}$ at E_{beam}=250,500 and 750 GeV by the ABEL simulation.

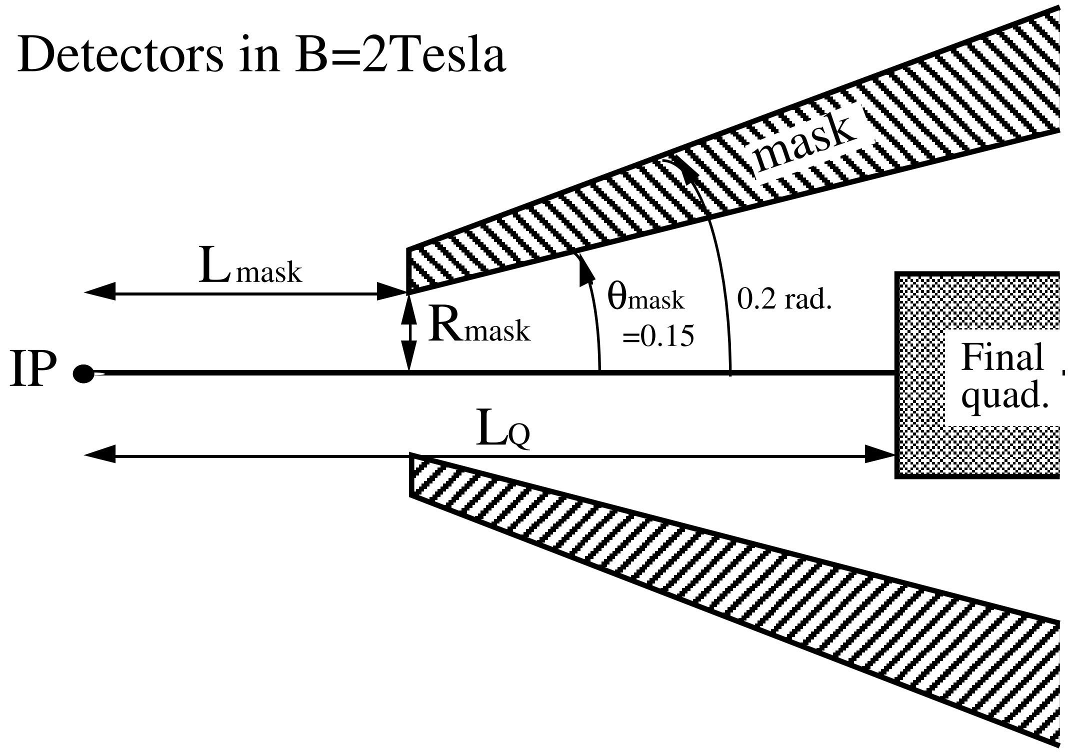

Figure 5: A masking system at the interaction region

4 Mask and Final Focus Quadrupole Magnet

Our masking system is schematically shown in Fig.5. As we fix the angular region of the mask as $0.15 < \theta_{mask} < 0.2$, it remains to determine only one parameter to fully specify the geometry of the mask. We take the half aperture of the mask, R_{mask} in Fig.5, for this parameter. R_{mask} can be linearly related to a diameter of circular trajectory of a charged track in a solenoidal magnetic field(B), *i.e.* $R_{mask} = p_t^{max}/0.15B$ and B=2Tesla.

In the previous study [10], R_{mask} has been set for all the pair particles created by the incoherent processes to loop inside the mask, where zero inherent angles have been assumed for the pairs. Here we determine R_{mask} in a similar way but for the pairs which comprise the shoulder in Fig.4. There is another important constraint from the solid angle seen by the photons back-scattered at the nearest final focus quadrupole magnet, *i.e.* $\eta_{mask} = R^2_{mask}/4(L_Q - L_{mask})^2 < 1 \times 10^{-3}$, where L_{mask} and L_Q are the distances of the mask and the final focus quadrupole magnet from the interaction point(IP), respectively(Fig.5). Therefore the location of the final focus quadrupole magnet can be optimized. As the kick angle of the pair, which is a major source of the p_t, depends on beam energy and beam spot size etc. , there are three corresponding parameter sets at $E_{beam} = 250, 500$ and 750 GeV as listed in Tab.3. With the masking system specified in this table, the total number of charged particles hitting the outer surface of the mask is less than 10^3/train(20 bunches) as shown in Fig.4. Outside the mask the number of pairs with $p_t > 0.2$ GeV is negligibly small at E_{beam} <500GeV and it is still O(1)/train at $E_{beam} = 750$GeV.

Table 3: Optimized parameters of the mask and the final focus quadrupole magnet at E_{beam}=250,500 and 750GeV assuming $\eta_{mask} = 10^{-3}$ and B=2Tesla.

E_{beam} GeV	p_t^{max} MeV	R_{mask} cm	L_{mask} m	L_Q m
250.	13.	4.5	0.3	1.0
500.	23.	7.7	0.51	1.7
750.	30.	10.0	0.67	2.2

5 Background at the Vertex Detector

Thus we designed the mask by considering the background of the back-scattered photons in the detector region. In general we can use a beampipe of small radius, e.g. $R_{pipe} <$ 1cm, at the IR because of no fear of synchrotron radiation [10]. Therefore, a vertex detector can be placed very close to the beam line. In order to estimate the background in the vertex detector, the number of hit points , which the pairs make by traversing the surface of the cylinder of radius R_{vtx} and length $Z_{vtx} = R_{vtx}/\tan\theta_{vtx}$ around the collision point, are plotted as a function of R_{vtx} at $|\cos\theta_{vtx}|$=0.707 and 0.9 at the three beam energies in Fig.6(a),(b). Here we assume the helix trajectories of the pairs in the solenoidal magnetic field of 2 Tesla and we allow for the pairs to register multiple hit points without any interaction. The number of hits decreases rapidly as R_{vtx} increases at E_{beam}=250 and 500GeV. However it remains almost constant between R_{vtx}= 5 and 10cm at E_{beam}=750GeV since curling tracks traverse the cylinder more times with a longer $Z_{vtx}(\propto R_{vtx})$. The hit numbers per bunch crossing are 16(36),60(136) and 123(296) at R_{vtx}=3cm, $|\cos\theta_{vtx}|$=0.707(0.9) for E_{beam}=250,500 and 750GeV, respectively, which have to be multiplied by 20 for a real background estimation because there are 20 bunches/train. This background apparently prevents us from using a gas chamber as the vertex detector in R_{vtx} <10cm. A pixel device can be a candidate detector. The vertex detector also suffers from the back-scattered photons. Since the number of these photons is on the order of 10^3 per train crossing, the corresponding hit number in the vertex detector is always less than those of the pairs with a few % of the conversion probability of the photons.

6 Summary

We derived analytic expressions of the integrated cross sections of the three incoherent processes as a function of x_t° and $\theta_\circ$. ABEL has been modified to include $e^\pm$ pair creation with inherent scattering angles in the real photon approximation. It also takes into account the three major effects, *i.e.* (1) the kick, (2) the geometric reduction and (3) the effect of the external field. In the angular region larger than the kick angle, the analytic calculations turned out to still be a good approximation to the simulation results if they were multiplied by a geometric reduction factor of about 40%. The aperture of the mask (R_{mask}) and the location of the final focus quadrupole magnet (L_Q) have been optimized at E_{beam}=250, 500 and 750GeV for JLC by using the ABEL simulation. R_{mask} was determined by the maximum transverse momentum due to the kick at θ_{mask}=0.15. Then L_Q was obtained from consideration on the solid angle, through which the back-scattered photons exit from the mask,*i.e.* $\eta_{mask} < 10^{-3}$. We had to move the final focus quadrupole magnet slightly

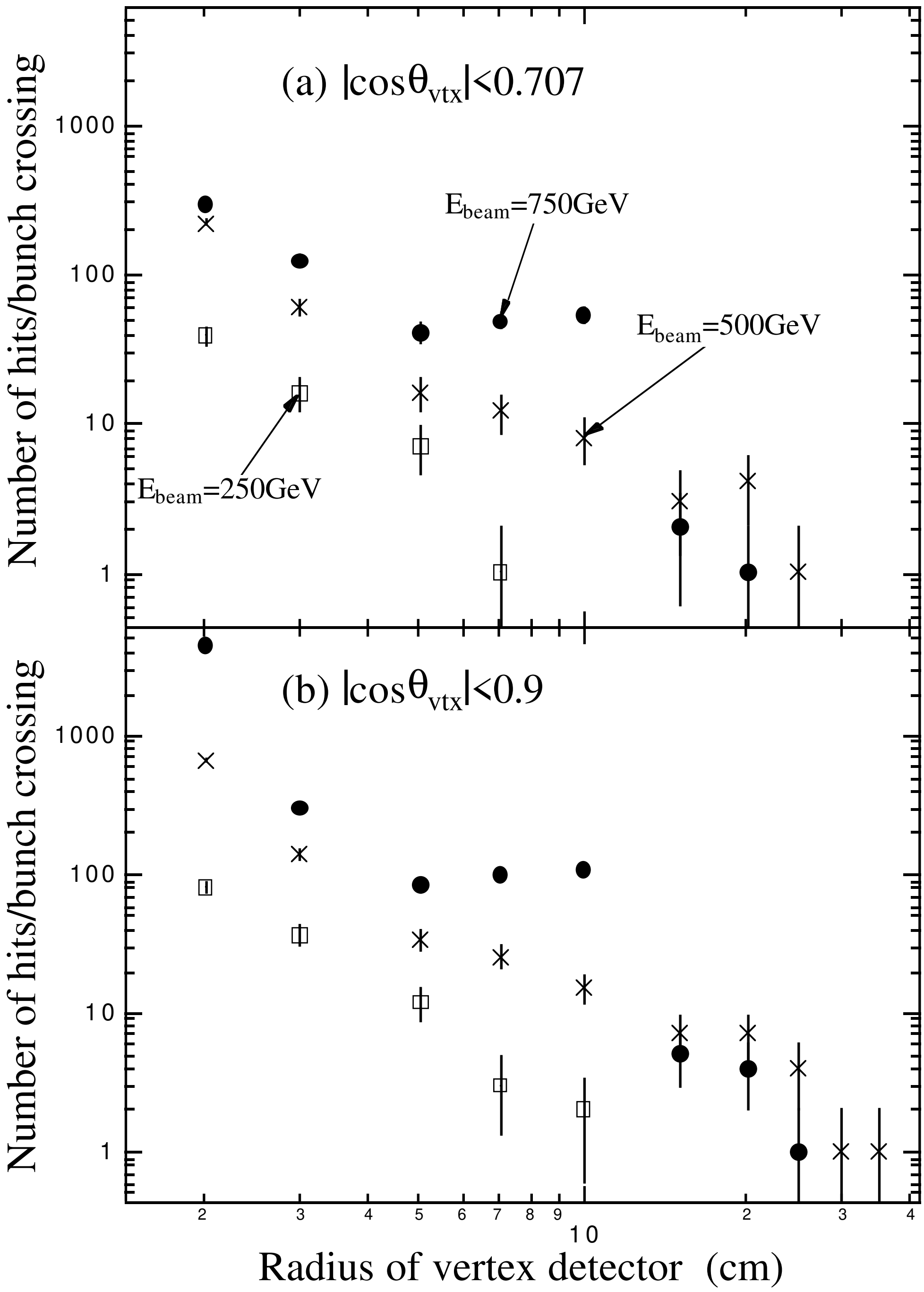

Figure 6: The number of hits in the vertex detector as a function of R_{vtx} for (a) $|\cos\theta_{vtx}| < 0.707$ and (b) $|\cos\theta_{vtx}| < 0.9$ at E_{beam}=250,500 and 750GeV, where the pair can have multiple hits because of the helical trajectory in B=2 Tesla.

away from the previous position, *i.e.* L_Q=2.2m at E_{beam}=750GeV. With this optimization there was no serious background problem in the major detector region of R >30cm and θ >0.2 . The background in the vertex detector ($3 < R_{vtx} < 10$cm) was also estimated to be $O(10^2) \sim O(10^3)$ hits made by the pairs at $E_{beam} = 250 \sim 750$ GeV. While a usual gas chamber can not survive as a vertex detector, a pixel type detector promises to work well in the presence of this many extra hits.

In conclusion, although an enormous number of $e^{\pm}$ pairs are created and kicked out during the beam-beam collision at the interaction region of JLC, we can execute an experiment without serious background problem by using the proper masking system. It is even possible to locate a vertex detector close to the beam, which has an essential role in efficient b-quark tagging.

References

[1] M. S. Zolotarev, E. A. Kuraev and V. G. Serbo, Inst. Yadernoi Fiziki Preprint 81-63 (1981); SLAC TRANS-227 (1987)

[2] P. Chen, T. Tauchi and D. V. Schroeder, “Pair Creation at Large Inherent Angles” Presented at the DPF Summer Study on High Energy Physics: Research Directions for the Decade, Snowmass, Colorado, June 25-July 13, 1990, SLAC-PUB-5652.

[3] K. Yokoya, ABEL,“A Computer Simulation Code for the Beam-Beam Interaction in Linear Colliders”, KEK-Report-85-9, Oct. 1985, also *Nucl. Instr. Meth.* **B251**, 1 (1986).

[4] V. B. Berestetskii, E. M. Lifshitz and L. P. Pitaevskii, *Relativistic Quantum Theory* , Part 1, Pergamon Press (1971).

[5] K. Yokoya, “Beam parameters for JLC” in the procceedings of LC91, protvino, Sep. 1991.

[6] G. L. Kotkin, S. I. Polityko and V. G. Serbo, *Sov. J. Nucl. Phys.* **42** , 440, (1985).

[7] A. E. Blinov, A. E. Bondar, Yu. I. Eidelman *et al.*, *Phys. Lett.* **113B**, 423 (1982). Yu. A. Tikhonov, *Candidates's Dissertation* , Inst. Nucl. Phys., Novosibirsk (1982).

[8] V. N. Baier, V. M. Katkov and V. M. Strakhovenko, *Sov. J. Nucl. Phys.* **36** , 95, (1982). A. I. Burov and Ya. S. Derbenev, INP Preprint 82-07, Novosibirsk (1982).

[9] V. N. Baier, V. M. Katkov, *Sov. Phys. Dokl.* **17** , 1068, (1973).

[10] T.Tauchi *et al.*, “Background Problem at Interaction Point for an e^+e^- TeV Linear Collider” Presented at the DPF Summer Study on High Energy Physics: Research Directions for the Decade, Snowmass, Colorado, June 25-July 13, 1990, SLAC-PUB-5652.